Develop an efficient and specific AAV-based labeling system for Muller glia in mice

Yanxia Gao[1,#], Kailun Fang[1,#], Zixiang Yan[2,#], Haiwei Zhang[1,#], Guannan Geng[1], Weiwei Wu[3], Ding Xu[4], Heng Zhang[5], Na Zhong[1], Qifang Wang[1], Minjing Cai[1], Erwei Zuo[2], Hui Yang[1,*]

[1]Institute of Neuroscience, CAS Center for Excellence in Brain Science and Intelligence Technology, Shanghai Research Center for Brain Science and Brain-Inspired Intelligence, Chinese Academy of Sciences, Shanghai, China.

[2]Shenzhen Branch, Guangdong Laboratory for Lingnan Modern Agriculture, Genome Analysis Laboratory of the Ministry of Agriculture, Agricultural Genomics Institute at Shenzhen, Chinese Academy of Agricultural Sciences, Shenzhen, China.

[3]Huigene Therapeutics Inc., Shanghai, China.

[4]Department of Vascular Surgery, Changhai Hospital, Navy Medical University, Shanghai, P.R. China.

[5]Department of Vascular Surgery, The Affiliated Hospital of Qingdao University, Qingdao, China.

[#]These authors contributed equally.

*Correspondence: huiyang@ion.ac.cn (H.Y.)

Abstract

Cell degeneration in the retina leads to several ocular diseases and vision loss. Considerable research efforts focus on reprogramming Muller glia (MG) into functional cells to rescue vision as a promising therapeutic strategy, although whether MG can convert into functional amacrine cells, bipolar cells, retinal ganglia cells (RGCs), rods or cones in mammals remains controversial. The broad applicability of tracking MG differentiation thus presents a need for improved labeling efficiency and specificity. Here, we compared AAV-based labeling strategies with conventional lineage-tracking by crossing transgenic mouse lines. We found that reporter expression was weak and not MG-specific in *mGFAP-Cre* transgenic mice. Different AAV serotypes showed a range of efficiency and specificity in labeling MG, leading us to optimize *a human GFAP-Cre* reporter system packaged in the AAV9 serotype with the *WPRE* (WPRE, woodchuck hepatitis virus post-transcriptional regulatory element) removed. The *hGFAP-Cre-* Δ*WPRE* reporter could label 20-73.8% MGs, with non-specific RGC labeling rates ranging from 0-0.08% at doses of 1 X 10^8 to 10^{10} vector genomes (vg) per eye, an approximate 40-fold reduction compared with the *AAV9-hGFAP-Cre-WPRE* labeling system. The *AAV9-hGFAP- Cre-*Δ*WPRE* system thus represents a highly efficient and specific labeling system for Muller glia, providing a valuable tool for tracking cell fate *in vivo*.

Introduction

Muller glia (MG) represents the main type of glial cell which are responsible for maintaining retinal structure and support for neurons in the retina. In lower vertebrates (e.g., zebrafish, *Danio rerio*), MG can re-enter the cell cycle to proliferate and subsequently

differentiate into one of multiple cell types following injury, such as photoreceptors or retinal ganglia cells (RGCs) (Bernardos, Barthel, Meyers, & Raymond, 2007; Fimbel, Montgomery, Burket, & Hyde, 2007; Goldman, 2014; Sherpa et al., 2008). However, the process does not occur in mammals. As a result, many ocular diseases that are difficult to treat, such as glaucoma or retinitis pigmentosa, develop from functional degeneration or loss of neurons. Thus, decades of research efforts have been committed to investigating the regenerative machinery in adult mammals with the ultimate goal of inducing MG regeneration and reprogramming. Several major insights have emerged from this work. For example, in mice Ascl1 overexpression or simultaneous deletion of three nuclear factors I (NFI) genes can both induce MG proliferation and transformation into amacrines or bipolar cells (Hoang et al., 2020; Ueki et al., 2015). Similarly, MG to conversion to RGCs was also observed in mice following deletion of Ptbp1 or simultaneous ectopic expression of Pou4f2 (Brn3b) and Atoh7 (Math5) (Xiao et al., 2021; Zhou et al., 2020). Moreover, photoreceptors could be generated from MG under simultaneous overexpression of Otx2, Crx and Nrl after a period of β-catenin ectopic expression (Yao et al., 2018).

However, *in vivo* glial lineage-tracing methods represent a long-standing research objective. For instance, an AAV-mediated glial reporter in the brain has been used by different research groups to observe the conversion of neuroD1-induced astrocytes into neurons (Boutin et al., 2010; Brulet et al., 2017; Chen et al., 2020; Wang et al., 2021). However, this phenomenon was not detectable using a more stringent, inducible, transgenic lineage-tracing strategy (Wang et al., 2021). One proposed explanation is that AAV-mediated reporters also non-specifically label neurons, suggesting that no conversion was observed, or alternatively, that inducible transgene methods cannot label all astrocytes, and thus do not label the resulting reprogrammed neurons. Similar confounding factors have been reported in MG lineage-tracing systems, such as the low or extremely variable labeling efficiency in inducible CreER mouse lines (Jorstad et al., 2017; Rueda et al., 2019; Thanh Hoang et al., 2021; Ueki et al., 2015), or potential non-specific labeling of other cell types by AAV-based methods, similar to the problems in astrocyte studies mentioned above (Yao et al., 2016; Yao et al., 2018). It is therefore crucial to develop an efficient and stringent tool for tracing MG proliferation and reprogramming in the retina.

Here, we compared the labeling efficiency and specificity of two different reporter systems: those based on crossing *mGFAP-Cre* transgenic mice and those based on transfection with AAV-*hGFAP-Cre* constructs in Ai9 mice, which harbor the *Rosa26-CAG-loxp-stop-loxp-tdTomato* inducible reporter. By optimizing the AAV reporters through WPRE (WPRE woodchuck hepatitis virus post-transcriptional regulatory element) cassette deletion, selecting the most suitable serotype, conducting immunofluorescence microscopy to quantify construct specificity and efficiency *in vivo*, we provide a novel, highly specific and reproducible labeling system for MG cells in the retina tissue of mice.

Result

MGs are not accurately labeled in *Ai9;mGFAP-Cre* mice

We first sought to test the specificity of MG labeling by *mGFAP-Cre* transgenic mouse, as reported in previous work to label astrocytes (Garcia, Doan, Imura, Bush, & Sofroniew, 2004). To this end, we generated an *Ai9;mGFAP-Cre* mouse line to label MGs (figure 1A) and found

that these tdTomato-labeled cells were distributed throughout the inner nuclear layer (INL) (Figure 1B, C), whereas MGs were distributed within a relatively tight layer in the middle of the INL (Figure 1B). Immunofluorescence staining showed the tdTomato reporter poorly labeled MGs, since only 6.42% ± 0.59% of total tdTomato$^+$ cells (501/7722) were co-labeled with the MG marker Sox9 (Figure 1D). However, we also found that a small proportion of tdTomato$^+$ cells scattered in the ganglia cell layer (GCL) (Figure 1B), and these cells did not strictly co-localize with the RGC markers Rbpms or Brn3a (i.e., only overlapped with each marker in five cells, or <2% of total RGCs, per eye section) (Figure 1E-F). Cumulatively, these results indicated that the endogenous GFAP-driven reporter did not leak to RGCs, nor accurately label MGs in this mouse line.

AAV-based reporter labels MGs efficiently but not specifically

AAV-based Cre expression is also commonly used to label MG cells in mice due to its relatively easier introduction compared to generating transgenic mouse lines (Xiao et al., 2021; Yao et al., 2016; Yao et al., 2018; Zhou et al., 2020). However, the efficiency of AAV-based labeling also depends on transfection efficiency, which can be affected by AAV serotype. To evaluate the labeling efficiency of different AAV serotypes, we packaged the *hGFAP-Cre-WPRE* construct into commonly used AAV vectors, including AAV1, AAV2, AAV5, AAV8, AAV9, and AAV.ShH10 (Buck & Wijnholds, 2020; Yao et al., 2018), and separately delivered them to the retinas of Ai9 mice by subretinal injection (Figure 2A). The results showed distinct patterns of transfection for the different serotypes. In particular, AAV1 and AAV5 showed less diffusion in the retina and their transfection area was smaller than that of other vectors, while AAV8 and AAV9 exhibited higher transfection efficiency than other vectors, with >500 labeled cells per section, on average (Figure 2B-D). Unexpectedly, the tdTomato reporter showed highly variable leakage (i.e., RGC labeling) among serotypes (Figure 2E). Notably, AAV2 and AAV.ShH10 labeled a greater number of RGCs (>50, or 10% of total tdTomato$^+$ cells on average per eye section) than other vectors (Figure 2F-G). These results implied that the selection of specific AAV serotypes could improve transfection efficiency, but could not prevent non-specific labeling of RGCs (or possibly other cell types). Thus, an alternative method was necessary to improve labeling specificity.

Deletion of the *WPRE* element in the AAV9 construct eliminates non-specific neuron labeling

Since *WPRE* is often used to enhance gene expression in AAV vectors (Challis et al., 2019; Choi et al., 2014; Deverman et al., 2016), we hypothesized that increasing Cre expression could lead to tdTomato activation in cells with low GFAP promoter activity, potentially resulting in non-specific labeling of RGCs by AAV-based reporters targeting MG. To test this hypothesis, we deleted *WPRE* from the reporter construct (Figure 3A) and packaged it in the AAV9 serotype for delivery by subretinal injection to the eyes of Ai9 mice. We then evaluated the efficiency and MG specificity of tdTomato$^+$ labeling. We found that transfection area and cell number varied in a dose dependent manner, with more extensive reporter signal in the high dose injection groups ($1x10^9$ and $1x10^{10}$ vector genomes /eye) and smaller transfection area and fewer labeled cells in the $1x10^8$ group (Figure 3B-C). However, transfection area and cell number were comparable between the *WPRE* and Δ*WPRE* groups at $1x10^9$ dose (Figure 3C). Among total tdTomato$^+$ cells, an average of 700 (73.8% ± 8.5%), 423 (51.6% ± 9.4%), and 153 (20% ± 4.16%) cells were co-labeled with the Sox9 marker in the

130 $1x10^{10}$, $1x10^{9}$, and $1x10^{8}$ groups, respectively, accounting for 99%, 98%, and 96% of the total
131 labeled cells separately (Figure3 E-F). These results indicated that deletion of *WPRE* could
132 keep the efficiency and improve the selectivity of in vivo MG labeling.
133 Moreover, tdTomato^{+}Rbpms^{+} cells were largely undetectable in each of the different AAV
134 dosage groups, even in high density tdTomato^{+} cells (Figure 3G), and with strong statistical
135 significance, since less than one RGC (15 tdTomato^{+}Rbpms^{+} cells in 22269 total labeled cells)
136 on average was labeled per eye section (Figure 3H-I). Under the same dose ($1x10^{9}$ vg/eye),
137 the Δ*WPRE* group showed a 40-fold reduction in the ratio of tdTomato^{+}Rbpms^{+} cells to total
138 tdTomato^{+} cells (from 3.93% ± 0.61% to 0.08% ± 0.05%), and an 80-fold (from 6.72% ± 1.15%
139 to 0.08% ± 0.04%) among total Rbpms^{+} cells (Figure 3H), compared with the *WPRE* group. It
140 warrants mention that the proportion of labeled RGCs remained consistently low across a wide
141 dosage range, 0.08% to 0% from $1x10^{10}$ to $1x10^{8}$ vg per eye in the Δ*WPRE* group. These
142 results indicated that the ΔWPRE AAV reporter system could labeled MGs with high specificity,
143 with only negligible staining of RGCs, even in experiments requiring high dose transfection.
144 We observed that a very small proportion of tdTomato^{+} cells were not labeled by Sox9
145 marker for MG (e.g., 9/431 in the $1x10^{9}$ group in one section, Figure 3G), leading us to
146 question whether these cells were other neuron types, such as bipolar cells, amacrine cells or
147 horizontal cells. To explore this possibility, we conducted immunofluorescent staining for
148 PKC-α (the bipolar cell marker), Calbindin (marked horizontal cells, amacrine cells and RGCs,
149 but could distinguish horizontal cells in mice) and Calretinin (mainly marked mouse amacrine
150 cells)(Kovacs-Oller et al., 2019; Liets, Eliasieh, van der List, & Chalupat, 2006) in eye sections
151 with tdTomato^{+} cells labeled by the Δ*WPRE*-AAV9 system and detected no co-labeling among
152 these cells (Figure S1A-D). Moreover, as shown in Figure 3D, in the outer nuclear layer (ONL)
153 composed of photoreceptors, tdTomato^{+} cells were not observed. Collectively, these results
154 indicated that this *AAV9-hGFAP-Cre-ΔWPRE* reporter system did not label other retina neuron
155 types either, which could be used to label MG with high specificity and at a wide dosage range
156 in Ai9 mouse retina.
157

158 ## Discussion

159 In this study, we developed a relatively straightforward and accessible mouse MG labeling
160 system in which AAV9-based *hGFAP-Cre-ΔWPRE* was applied in Ai9 transgenic mice. This
161 system can label MG efficiently and specifically without obvious mislabeling of other functional
162 neurons, including RGC, photoreceptors, amacrines, bipolar and horizontal cells.
163 Selecting an appropriate system for tracking MG in vivo is essential for investigations of
164 MG reprogramming. While the introduction of reporters by crossing with a transgenic Cre
165 mouse line provides more consistent and stable labeling than AAV-based systems, the labeling
166 efficiency may be low. In this study, we found that introduction of the *mGFAP-Cre* transgenic
167 construct by conventional crossing failed to label the majority of MGs, unlike that reported for
168 astrocytes in brain tissues (Garcia et al., 2004). Mouse lines with inducible Cre, such as
169 CreER, are considered more stringent than constitutive Cre lines, but the labeling efficiency is
170 dependent on tamoxifen dose (Hu et al., 2020), and was shown to exhibit particularly low
171 effectiveness in tracking MG in other studies (Jorstad et al., 2017; Ueki et al., 2015).
172 Additionally, tamoxifen administration reportedly impairs neurogenesis (C. M. Lee et al., 2020)
173 and can adversely affect the activity and specificity of promoters driving Cre (Denk et al., 2015;

174 Donocoff, Teteloshvili, Chung, Shoulson, & Creusot, 2020).
175 Considering the heterogeneity of MGs including many subtypes (Menon et al., 2019;
176 Roesch et al., 2008), conclusions regarding the ability of MG to differentiate into other
177 neuronal types require validation by labeling and detection of all MG subtypes. However, the
178 labeling efficiency of MG by AAV-based reporters primarily depends on its transfection
179 efficiency which can be affected by AAV tropisms, enhancer elements in the Cre vector (such
180 as *WPRE*), and injection methods. The AAV1, 2, 5, 8, 9 and ShH10 serotypes with an eGFP
181 reporter driven by CMV or CAG promoters have been shown to transfect MG using intravitreal
182 or subretinal injection (Klimczak, Koerber, Dalkara, Flannery, & Schaffer, 2009; Lebherz,
183 Maguire, Tang, Bennett, & Wilson, 2008; Surace et al., 2003). We compared the transfection
184 patterns of these serotypes using an *hGFAP-Cre* vector and found that AAV1, AAV2, or AAV5
185 were ineffective for MG transfection. Other recent work showed variable specificity by different
186 serotypes for labeling astrocytes in the brain (Wang et al., 2021), which were in line with our
187 results in the retina.
188 In addition, high specificity for tracking MG is indispensable for exclusion of false-positive
189 results in investigation of MG conversion to neurons. Until now, the efficiency and specificity of
190 AAV-based labeling of astrocytes remains controversial for study of neurogenesis and
191 reprogramming, especially in the brain (Thanh Hoang et al., 2021; Wang et al., 2021). We
192 found that all serotypes exhibited varying degrees of leakage to RGCs in the retina. We further
193 improved the vector by removing the *WPRE* element and found that labeling efficiency was not
194 obviously affected, but the proportion of non-specifically labeled cells decreased by at least
195 40-fold that of systems which include *WPRE,* substantially lower than that of other reported
196 tracking systems for astrocytes in the brain (Srinivasan et al., 2016; Wang et al., 2021).
197 Moreover, the system lacking *WPRE* exhibits a consistently low non-specific labeling ratio
198 across a wide dose range, from $1x10^8$ to $1x10^{10}$ vg per eye, suggesting its potential reliability
199 for tracking MG.
200 However, the specificity of this AAV-mediated reporter system depends on MG-specific Cre
201 expression driven by the GFAP promoter. If the manipulated gene of interest affects GFAP
202 promoter activity, its overexpression or knockdown in other cell types, such as neurons, may
203 activate the GFAP promoter and initiate Cre expression in those neurons, in turn affecting its
204 specificity for MG. For example, NEUROD1 may function as a *cis*-regulator of the *hGFAP*
205 promoter (Wang et al., 2021). Under this condition, other tracking strategies, such as labeling
206 neurons with retrograde virus (Wang et al., 2021), may need to be combined with this method
207 to further validate the results. In all, our AAV9 *hGFAP-Cre-ΔWPRE* system could offer
208 conveniences for fundamental research in vertebrate eye development, as well as the
209 potential for development of MG-targeted therapeutics.
210

211 ## Materials and methods

212 ### Animals

213 All mice were housed under a 12 hour light/dark cycle with water and food provided *ad*
214 *libitum* at the Animal Center of the Institute of Neuroscience, Chinese Academy of Sciences,
215 Shanghai, China. All animal procedures were approved by the Animal Care and Use
216 Committee. All reporters were based on tdTomato expression in Ai9 transgenic mice
217 (*CAG-Loxp-stop-Loxp-tdTomato*, JAX #007909) purchased from the Jackson Laboratory.

GFAP-Cre (B6.Cg-Tg(Gfap-cre)73.12Mvs/J, JAX#012886) mice were gifted by Dr. Jiawei Zhou in the Institute of Neuroscience, Chinese Academy of Sciences.

AAVs and vectors

AAV vectors, *hGFAP-Cre-ΔWPRE,* and *hGFAP-Cre-WPRE* were constructed by PCR-based subcloning. The 681-bp human GFAP promoter was used in this study, which was derived from the 2.2-kb gfa2 promoter (Y. Lee, Messing, Su, & Brenner, 2008). Different serotypes of AAVs were packaged and titered by Gene Editing Core Facility in the Institute of Neuroscience.

Subretinal and intravitreal injection

AAVs were delivered to eyes via subretinal injection, as previously described (Chiu, Chang, & So, 2007; Qi et al., 2015). For subretinal injection, adult mice were anaesthetized with a mixture of ketamine and xylazine, and pupils were dilated with tropicamide phenylephrine eye drops before injection. A small scleral incision was made using a 30G needle under a microscope (Olympus, Tokyo, Japan). Then a 32G needle on a Hamilton syringe was inserted into the subretinal space though the scleral incision. 1 μl of AAV was slowly (i.e., up to 20s) injected into the subretinal space. After AAV injection, the Hamilton syringe was removed and a drop of ofloxacin eye ointment was applied to cover the eye.

Immunofluorescent staining and Imaging

Mouse eyes were collected after perfusing animals with 4% paraformaldehyde (PFA) in PBS, and post-fixed for half an hour in PFA at room temperature after removing the cornea. Then, retinas were dissected and dehydrated overnight using 30% (*w/v*) sucrose in PBS and embedded in O.C.T (Sakura). Sections were performed by a cryostat (HM525, Thermo).

Before staining, sections were dried for 30 minutes at 65℃ and then were washed in PBS 3 times for 5 minutes per wash. Antigen recovery was performed using heated sodium citrate. Blocking was performed in 150 μl blocking buffer (0.1 M PBS: 10% goat serum, and 0.1% Tween-20). Primary antibodies were incubated at 4℃ overnight. Details of primary antibodies used in this study were as follows: rabbit anti-Rbpms (1:200, Proteintech, 15187-1-AP), mouse anti-Brn3a (1:100, Millipore, MAB1585), mouse anti-Sox9 (1:200, Sigma, Amab90795), rabbit anti-Rfp (1:200, Rockland, 600-401-379), Mouse-anti-PKC α (1:200, Santa Cruz Biotechnology, sc-8393), Rabbit-anti-Calbindin (1:200, Proteintech, 14479-1-AP) and mouse-anti-Calretinin (1:200, Proteintech, 66496-L-IG). Sections were washed 3x for 10 minutes per wash on the second day. Secondary antibodies were also incubated at 4 ℃ overnight. These secondary antibodies included: Alexa Fluor 647-AffiniPure goat anti-mouse IgG (H+L) (1:500, Jackson ImmunoResearch, 115-605-003), Alexa Fluor 647-AffiniPure goat anti-rabbit IgG (H+L) (1:500, Jackson ImmunoResearch, 111-605-003), Fluorescein (FITC) AffiniPure goat anti-mouse IgG (H+L) (1:500, Jackson ImmunoResearch, 115-095-003), Cy™3 AffiniPure goat anti-rabbit IgG (H+L) (1:500, Jackson ImmunoResearch, 111-165-003). Sections were washed 3x for 10 minutes per wash on the third day. After nucleic DNA staining by 4′,6-diamidino-2-phenylindole (DAPI), sections were mounted with fluorescent anti-fade mounting medium (Southern Biotech, 0100-01). All sections were imaged by confocal microscopy (Olympus, FV3000). Images were processed using ImageJ.

Acknowledgements

We thank Dr. J. Zhou for offering transgenic *mGFAP-Cre* mouse line, X. Hu from H. Zhou

laboratory for discussion about plasmid construction, the Optical Imaging facility, Y. Wang, Y. Zhang and Q.Hu in ION. We thank Isaac V. Greenhut for discussions and comments on this manuscript. This work was supported by the Basic Frontier Scientific Research Program of Chinese Academy of Sciences From 0 to 1 original innovation project (grant no. ZDBS-LY-SM001), the R&D Program of China (grant no. 2017YFC1001300 and 2018YFC2000100), the CAS Strategic Priority Research Program (grant no. XDB32060000), the National Natural Science Foundation of China (grant nos. 31871502, 31925016, 91957122, 31901047, 82001355), the Shanghai Municipal Science and Technology Major Project (grant no. 2018SHZDZX05), the Shanghai City Committee of Science and Technology Project (grant nos. 18411953700, 18JC1410100, 19XD1424400, 19YF1455100) and the International Partnership Program of Chinese Academy of Sciences (grant no. 153D31KYSB20170059).

Author contributions

Y.G., K.F., Z.Y. and H.Y. conceived the project. Y.G., K.F., Z.Y. and H.Z. designed and conducted experiments. W. W. and G.G. assisted with virus package. D.X. and H.Z. performed cryostat section for retinas. N.Z., Q.W. and M.C assisted with animal experiments. H.Y. designed experiments and supervised the whole project. Y.G., K.F., Z.Y. and H.Y. wrote the paper.

Declaration of interests

The authors declare no competing interests.

References

Bernardos, R. L., Barthel, L. K., Meyers, J. R., & Raymond, P. A. (2007). Late-stage neuronal progenitors in the retina are radial Muller glia that function as retinal stem cells. *J Neurosci, 27*(26), 7028-7040. doi:10.1523/JNEUROSCI.1624-07.2007

Boutin, C., Hardt, O., de Chevigny, A., Core, N., Goebbels, S., Seidenfaden, R., . . . Cremer, H. (2010). NeuroD1 induces terminal neuronal differentiation in olfactory neurogenesis. *Proc Natl Acad Sci U S A, 107*(3), 1201-1206. doi:10.1073/pnas.0909015107

Brulet, R., Matsuda, T., Zhang, L., Miranda, C., Giacca, M., Kaspar, B. K., . . . Hsieh, J. (2017). NEUROD1 Instructs Neuronal Conversion in Non-Reactive Astrocytes. *Stem Cell Reports, 8*(6), 1506-1515. doi:10.1016/j.stemcr.2017.04.013

Buck, T. M., & Wijnholds, J. (2020). Recombinant Adeno-Associated Viral Vectors (rAAV)-Vector Elements in Ocular Gene Therapy Clinical Trials and Transgene Expression and Bioactivity Assays. *Int J Mol Sci, 21*(12). doi:10.3390/ijms21124197

Challis, R. C., Ravindra Kumar, S., Chan, K. Y., Challis, C., Beadle, K., Jang, M. J., . . . Gradinaru, V. (2019). Systemic AAV vectors for widespread and targeted gene delivery in rodents. *Nat Protoc, 14*(2), 379-414. doi:10.1038/s41596-018-0097-3

Chen, Y. C., Ma, N. X., Pei, Z. F., Wu, Z., Do-Monte, F. H., Keefe, S., . . . Chen, G. (2020). A NeuroD1 AAV-Based Gene Therapy for Functional Brain Repair after Ischemic Injury through In Vivo Astrocyte-to-Neuron Conversion. *Molecular Therapy, 28*(1), 217-234. doi:10.1016/j.ymthe.2019.09.003

Chiu, K., Chang, R. C., & So, K. F. (2007). Intravitreous injection for establishing ocular diseases model. *J Vis Exp*(8), 313. doi:10.3791/313

306 Choi, J. H., Yu, N. K., Baek, G. C., Bakes, J., Seo, D., Nam, H. J., . . . Kaang, B. K. (2014).
307 Optimization of AAV expression cassettes to improve packaging capacity and
308 transgene expression in neurons. *Mol Brain, 7*, 17. doi:10.1186/1756-6606-7-17
309 Denk, F., Ramer, L. M., Erskine, E. L., Nassar, M. A., Bogdanov, Y., Signore, M., . . . Ramer, M.
310 S. (2015). Tamoxifen induces cellular stress in the nervous system by inhibiting
311 cholesterol synthesis. *Acta Neuropathol Commun, 3*, 74.
312 doi:10.1186/s40478-015-0255-6
313 Deverman, B. E., Pravdo, P. L., Simpson, B. P., Kumar, S. R., Chan, K. Y., Banerjee, A., . . .
314 Gradinaru, V. (2016). Cre-dependent selection yields AAV variants for widespread
315 gene transfer to the adult brain. *Nat Biotechnol, 34*(2), 204-209. doi:10.1038/nbt.3440
316 Donocoff, R. S., Teteloshvili, N., Chung, H., Shoulson, R., & Creusot, R. J. (2020).
317 Optimization of tamoxifen-induced Cre activity and its effect on immune cell
318 populations. *Sci Rep, 10*(1), 15244. doi:10.1038/s41598-020-72179-0
319 Fimbel, S. M., Montgomery, J. E., Burket, C. T., & Hyde, D. R. (2007). Regeneration of inner
320 retinal neurons after intravitreal injection of ouabain in zebrafish. *J Neurosci, 27*(7),
321 1712-1724. doi:10.1523/JNEUROSCI.5317-06.2007
322 Garcia, A. D., Doan, N. B., Imura, T., Bush, T. G., & Sofroniew, M. V. (2004). GFAP-expressing
323 progenitors are the principal source of constitutive neurogenesis in adult mouse
324 forebrain. *Nature Neuroscience, 7*(11), 1233-1241. doi:10.1038/nn1340
325 Goldman, D. (2014). Muller glial cell reprogramming and retina regeneration. *Nat Rev*
326 *Neurosci, 15*(7), 431-442. doi:10.1038/nrn3723
327 Hoang, T., Wang, J., Boyd, P., Wang, F., Santiago, C., Jiang, L., . . . Blackshaw, S. (2020).
328 Gene regulatory networks controlling vertebrate retinal regeneration. *Science*.
329 doi:10.1126/science.abb8598
330 Hu, N. Y., Chen, Y. T., Wang, Q., Jie, W., Liu, Y. S., You, Q. L., . . . Gao, T. M. (2020).
331 Expression Patterns of Inducible Cre Recombinase Driven by Differential
332 Astrocyte-Specific Promoters in Transgenic Mouse Lines. *Neurosci Bull, 36*(5),
333 530-544. doi:10.1007/s12264-019-00451-z
334 Jorstad, N. L., Wilken, M. S., Rimes, W. N. G., Wohl, S. G., VandenBosch, L. S., Yoshimatsu,
335 T., . . . Reh, T. A. (2017). Stimulation of functional neuronal regeneration from Muller
336 glia in adult mice. *Nature, 548*(7665), 103-+. doi:10.1038/nature23283
337 Klimczak, R. R., Koerber, J. T., Dalkara, D., Flannery, J. G., & Schaffer, D. V. (2009). A novel
338 adeno-associated viral variant for efficient and selective intravitreal transduction of rat
339 Muller cells. *Plos One, 4*(10), e7467. doi:10.1371/journal.pone.0007467
340 Kovacs-Oller, T., Szarka, G., Ganczer, A., Tengolics, A., Balogh, B., & Volgyi, B. (2019).
341 Expression of Ca(2+)-Binding Buffer Proteins in the Human and Mouse Retinal
342 Neurons. *Int J Mol Sci, 20*(9). doi:10.3390/ijms20092229
343 Lebherz, C., Maguire, A., Tang, W., Bennett, J., & Wilson, J. M. (2008). Novel AAV serotypes
344 for improved ocular gene transfer. *J Gene Med, 10*(4), 375-382. doi:10.1002/jgm.1126
345 Lee, C. M., Zhou, L., Liu, J., Shi, J., Geng, Y., Liu, M., . . . Lin, Q. (2020). Single-cell RNA-seq
346 analysis revealed long-lasting adverse effects of tamoxifen on neurogenesis in
347 prenatal and adult brains. *Proc Natl Acad Sci U S A, 117*(32), 19578-19589.
348 doi:10.1073/pnas.1918883117
349 Lee, Y., Messing, A., Su, M., & Brenner, M. (2008). GFAP promoter elements required for

region-specific and astrocyte-specific expression. *Glia, 56*(5), 481-493. doi:10.1002/glia.20622

Liets, L. C., Eliasieh, K., van der List, D. A., & Chalupat, L. M. (2006). Dendrites of rod bipolar cells sprout in normal aging retina. *Proceedings Of the National Academy Of Sciences Of the United States Of America, 103*(32), 12156-12160. doi:10.1073/pnas.0605211103

Menon, M., Mohammadi, S., Davila-Velderrain, J., Goods, B. A., Cadwell, T. D., Xing, Y., . . . Hafler, B. P. (2019). Single-cell transcriptomic atlas of the human retina identifies cell types associated with age-related macular degeneration. *Nat Commun, 10*. doi:ARTN 4902

10.1038/s41467-019-12780-8

Qi, Y., Dai, X., Zhang, H., He, Y., Zhang, Y., Han, J., . . . Pang, J. (2015). Trans-Corneal Subretinal Injection in Mice and Its Effect on the Function and Morphology of the Retina. *Plos One, 10*(8), e0136523. doi:10.1371/journal.pone.0136523

Roesch, K., Jadhav, A. P., Trimarchi, J. M., Stadler, M. B., Roska, B., Sun, B. B., & Cepko, C. L. (2008). The transcriptome of retinal Muller glial cells. *Journal of Comparative Neurology, 509*(2), 225-238. doi:10.1002/cne.21730

Rueda, E. M., Hall, B. M., Hill, M. C., Swinton, P. G., Tong, X. F., Martin, J. F., & Poche, R. A. (2019). The Hippo Pathway Blocks Mammalian Retinal Muller Glial Cell Reprogramming. *Cell Reports, 27*(6), 1637-+. doi:10.1016/j.celrep.2019.04.047

Sherpa, T., Fimbel, S. M., Mallory, D. E., Maaswinkel, H., Spritzer, S. D., Sand, J. A., . . . Stenkamp, D. L. (2008). Ganglion cell regeneration following whole-retina destruction in zebrafish. *Dev Neurobiol, 68*(2), 166-181. doi:10.1002/dneu.20568

Srinivasan, R., Lu, T. Y., Chai, H., Xu, J., Huang, B. S., Golshani, P., . . . Khakh, B. S. (2016). New Transgenic Mouse Lines for Selectively Targeting Astrocytes and Studying Calcium Signals in Astrocyte Processes In Situ and In Vivo. *Neuron, 92*(6), 1181-1195. doi:10.1016/j.neuron.2016.11.030

Surace, E. M., Auricchio, A., Reich, S. J., Rex, T., Glover, E., Pineles, S., . . . Bennett, J. (2003). Delivery of adeno-associated virus vectors to the fetal retina: impact of viral capsid proteins on retinal neuronal progenitor transduction. *Journal Of Virology, 77*(14), 7957-7963. doi:10.1128/jvi.77.14.7957-7963.2003

Thanh Hoang, Dong Won Kim, Haley Appel, Nicole A. Pannullo, Manabu Ozawa, Sika Zheng, . . . Blackshaw, S. (2021). Ptbp1 deletion does not induce glia-to-neuron conversion in adult mouse retina and brain. *bioRxiv*.

Ueki, Y., Wilken, M. S., Cox, K. E., Chipman, L., Jorstad, N., Sternhagen, K., . . . Reh, T. A. (2015). Transgenic expression of the proneural transcription factor Ascl1 in Muller glia stimulates retinal regeneration in young mice. *Proceedings Of the National Academy Of Sciences Of the United States Of America, 112*(44), 13717-13722. doi:10.1073/pnas.1510595112

Wang, L. L., Serrano, C., Zhong, X., Ma, S., Zou, Y., & Zhang, C. L. (2021). Revisiting astrocyte to neuron conversion with lineage tracing in vivo. *Cell, 184*(21), 5465-5481 e5416. doi:10.1016/j.cell.2021.09.005

Xiao, D., Jin, K., Qiu, S., Lei, Q., Huang, W., Chen, H., . . . Xiang, M. (2021). In vivo Regeneration of Ganglion Cells for Vision Restoration in Mammalian Retinas. *Front*

Cell Dev Biol, 9, 755544. doi:10.3389/fcell.2021.755544

Yao, K., Qiu, S., Tian, L., Snider, W. D., Flannery, J. G., Schaffer, D. V., & Chen, B. (2016). Wnt Regulates Proliferation and Neurogenic Potential of Muller Glial Cells via a Lin28/let-7 miRNA-Dependent Pathway in Adult Mammalian Retinas. *Cell Reports, 17*(1), 165-178. doi:10.1016/j.celrep.2016.08.078

Yao, K., Qiu, S., Wang, Y. V., Park, S. J. H., Mohns, E. J., Mehta, B., . . . Chen, B. (2018). Restoration of vision after de novo genesis of rod photoreceptors in mammalian retinas. *Nature, 560*(7719), 484-+. doi:10.1038/s41586-018-0425-3

Zhou, H. B., Su, J. L., Hu, X. D., Zhou, C. Y., Li, H., Chen, Z. R., . . . Yang, H. (2020). Glia-to-Neuron Conversion by CRISPR-CasRx Alleviates Symptoms of Neurological Disease in Mice. *Cell, 181*(3), 590-+. doi:10.1016/j.cell.2020.03.024

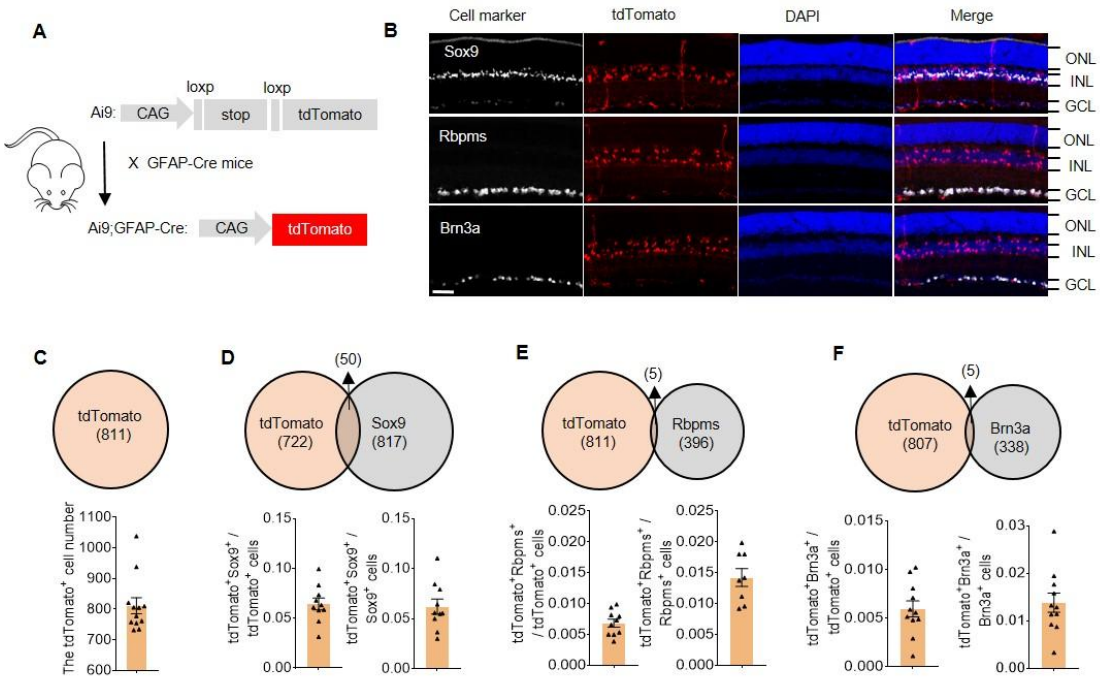

Figure 1 Muller glia are not well-labeled in the *Ai9;mGFAP-Cre* mouse line

(A) Schematic illustration of constructs used to establish the *Ai9;mGFAP-Cre* mouse line.

(B) tdTomato reporter co-localization with cell markers in *Ai9;mGFAP-Cre* mice. Rbpms and Brn3a are RGC markers; Sox9 specifically labels Muller glia (MG) in the retina. The tdTomato reporter is weakly co-expressed with these cell markers, which indicates poor labeling of MG by tdTomato and no detection of leakage to RGCs. Scale Bar, 50 μm. RGC, retinal ganglia cell; ONL, outer nuclear layer; INL, inner nuclear layer; GCL, ganglia cell layer.

(C) The tdTomato cell number in each eye section. n = 12 retinas per group.

(D-F) Venn diagram of average number of tdTomato-labeled cells and/or other cell markers in each section. n = 12 retinas per group. All values are presented as means ± S.E.M..

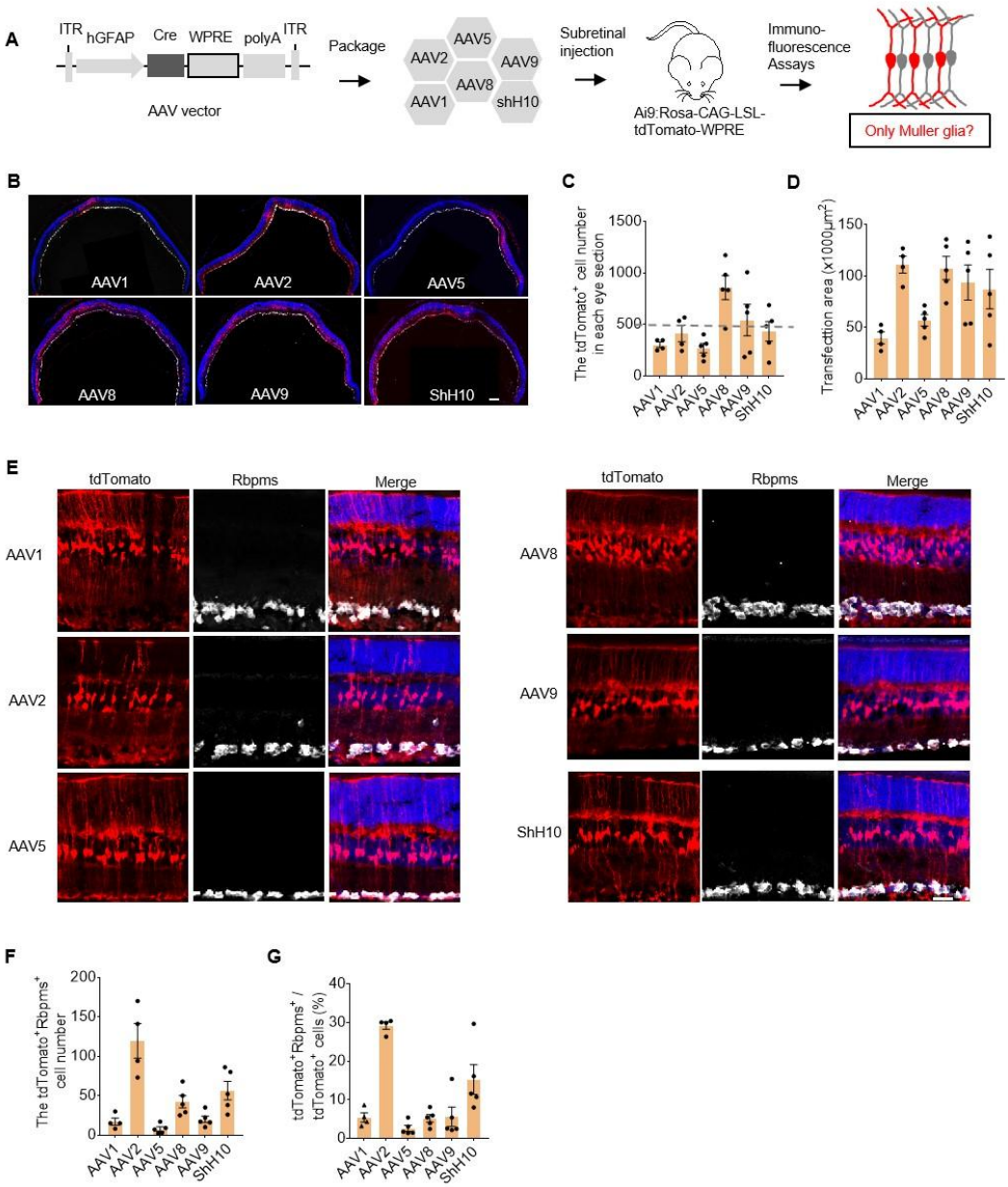

Figure 2 AAV-based systems co-label a small proportion of RGCs along with MG

(A) Schematic illustration of experimental design. Cre expression is driven by the human GFAP promoter and enhanced by the WPRE element. WPRE, woodchuck hepatitis virus post-transcriptional regulatory element.

(B) Representative images of transfection with different AAV serotypes through subretinal injection. Scale bar, 200 μm.

(C) The average number of tdTomato-labeled cells in each eye section infected by different AAVs.

(D) Quantification of transfection area in each section.

(E) Representative images of co-localization of tdTomato signal with Rbpms in the retina for each AAV serotype. Scale Bar, 50 μm.

(F) The number of tdTomato-labeled RGCs.

(G) The ratio of tdTomato-labeled RGCs to total labeled cells. n = 4~5 retinas per group for panels C, D, F and G. All values are presented as means ± S.E.M.

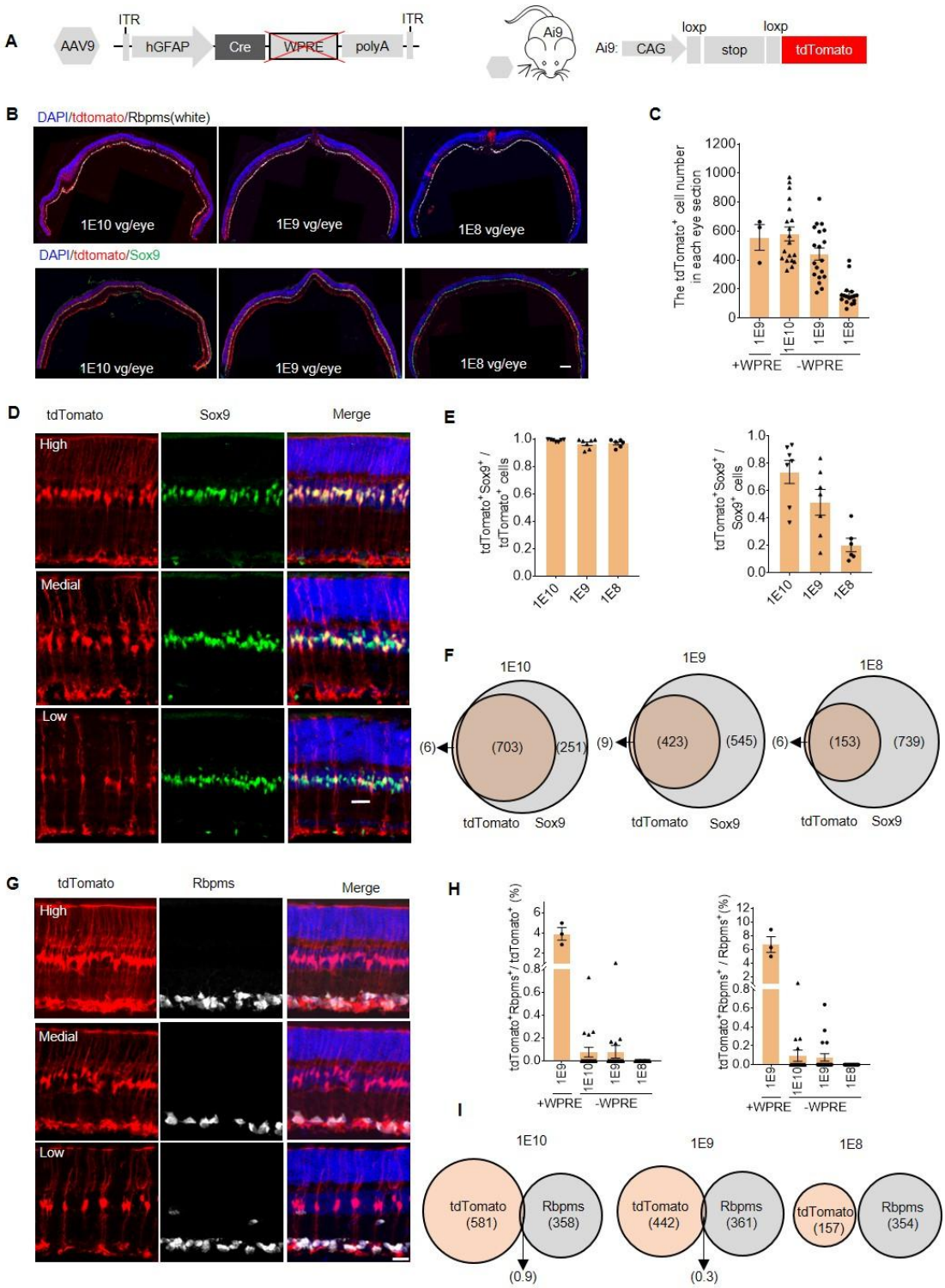

Figure 3 Reduced non-specific labeling in the ΔWPRE system

(A) Schematic diagram of the *hGFAP-Cre-ΔWPRE* vector and the tdTomato reporter construct in the Ai9 mouse line.

(B) Representative images of tdTomato co-localization with the Muller glia marker Sox9 in mouse retinas following subretinal injection with different doses of AAVs (from left to right:$1x10^{10}$, $1x10^{9}$, $1x10^{8}$ vector genomes per eye, vg/eye). Scale bar, 200 μm.

(C) The average number of tdTomato⁺ cells in each eye section infected by different doses of

AAVs.

(D) Representative images of tdTomato co-labeling with the Sox9 MG marker in different densities of labeled MG in retina sections. Scale Bar, 50 μm.

(E) The ratio of tdTomato-labeled MG among total labeled cells (left) and MG (right).

(F) Venn diagram of the average number tdTomato-labeled cells and MG in each section.

(G) Representative images of MG cells in retina sections co-labeled with tdTomato and RGC marker Rbpms in different transfection densities. Scale Bar, 50 μm.

(H) The ratio of tdTomato-labeled RGCs among total reporter cells (left) and RGCs (right).

(I) The Venn diagram of average tdTomato-labeled cells and RGCs in each section.

n = 3~7 retinas per group for panel C, E, H. All values are presented as means ± S.E.M..

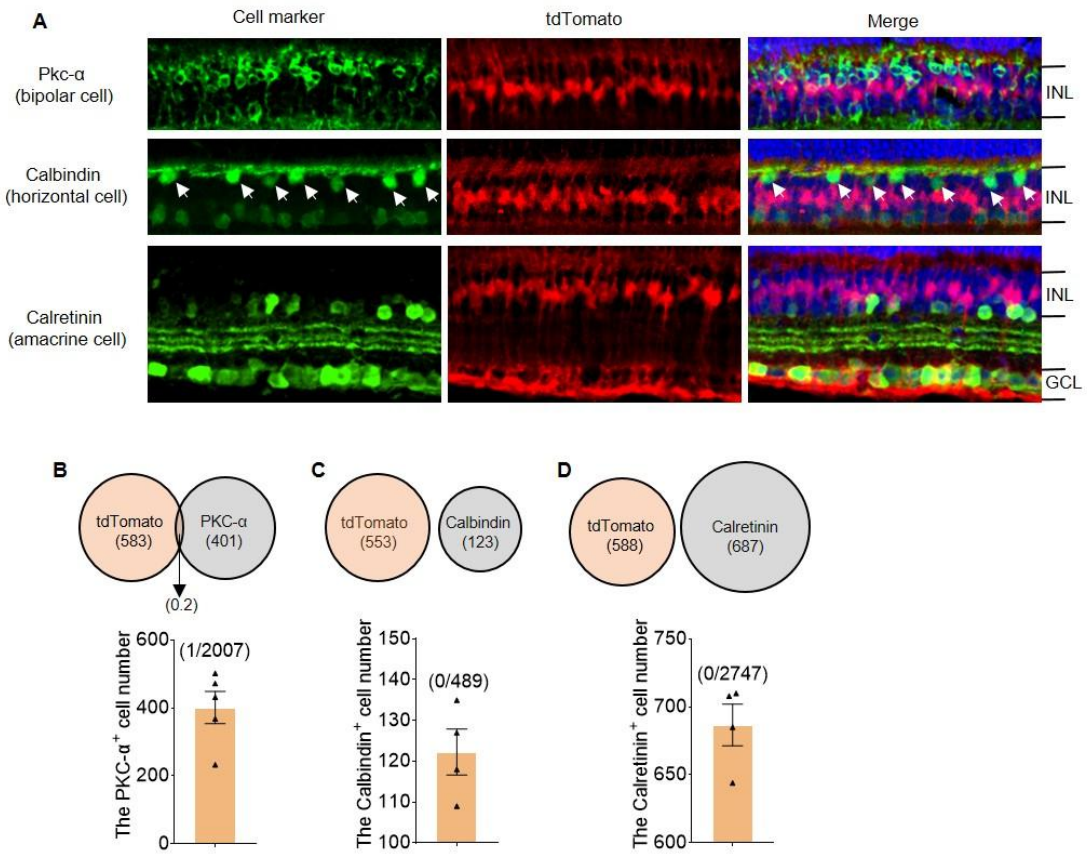

Figure S1 Reduced leakage in the ΔWPRE system related to Figure 3

(A) Co-localization of tdTomato and bipolar cell marker PKC-α, horizontal cell marker Calbindin and amacrine cell marker Calretinin. Arrows show horizontal cells. INL, inner nuclear layer. Scale Bar, 50 μm.

(B-D) Venn diagram of average tdTomato reporter and cell markers in each section (up); the number of PKC-α$^+$ (C), Calbindin$^+$ (C) and Calretinin$^+$ (D) cells in each eye section infected at 10^9 vg/eye (down). PKC-α marked bipolar cells, Calbindin marked horizontal cells, amacrine cells and RGCs in mice but could distinguish horizontal cells, pointed out by arrows) and Calretinin mainly marked mouse amacrine cells. Brackets show the number of both tdTomato and cell marker positive cells among total cell marker positive cells.

n=4~5 retinas for panel B-D. All values are presented as means ± S.E.M..